

Supporting Information

**Development of thiocyanate-free, charge-neutral Ru(II) sensitizers for
dye-sensitized solar cells**

Kuan-Lin Wu,^a Hui-Chu Hsu,^a Kellen Chen,^a Yun Chi,^{*,a} Min-Wen Chung,^b Wei-Hsin
Liu,^b Pi-Tai Chou^{*,b}

K.-L. Wu, H.-C. Hsu, K. Chen , Prof. Y. Chi

Department of Chemistry,

National Tsing Hua University, Hsinchu 300 (Taiwan)

Fax: (+886)3572-0864; E-mail: ychi@mx.nthu.edu.tw

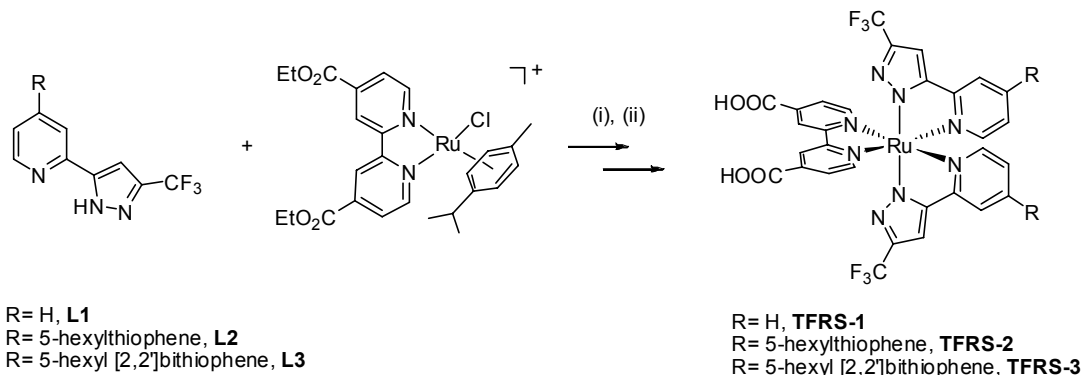
M.-W. Chung, Prof. P.-T. Chou, W.-H. Liu

Department of Chemistry,

National Taiwan University, Taipei 106 (Taiwan)

Fax: (+886)2-2369-5208; E-mail: chop@ntu.edu.tw

Experimental



Reaction conditions: (i) 2-methoxyethanol, 130°C, 12h (ii) acetone, NaOH, reflux, 2h.

Synthesis of TFRS-1

2-(3-(Trifluoromethyl)-1H-pyrazol-5-yl)pyridine (45mg, 0.21 mmol) and [Ru(4,4'-bis(ethoxycarbonyl)-2,2'-bipyridine)(*p*-cymene)Cl]Cl (60 mg, 0.10 mmol) were dissolved in 2-methoxyethanol (20 mL), and the reaction mixture was heated to 130 °C under stirring for 12 h. After evaporating the solvent, the aqueous phase was separated and extracted with dichloromethane (3 x 25 mL). The crude compound was purified by silica gel column chromatography ($\text{CH}_2\text{Cl}_2/\text{EtOAc} = 5:1$) . Finally, the resulting solid was dissolved in a mixture of acetone (5 mL) and 1M sodium hydroxide (5 mL). The solution was heated to 100 °C under N_2 for 24 h. After completing the hydrolysis, the solvent was removed and solid was dissolved in basic H_2O solution (10 mL) and was titrated with 2 M HCl to pH 3 to afford a brown precipitate. This brown product was then taken into a minimum amount of methanol and purified on Sephadex LH-20 column using methanol as the eluent. The main band was collected and solvent was evaporated to dryness. After then, the brown precipitate was washed with deionized water and diethyl ether in sequence, giving **TFRS-1** as powdery material (25 mg, 32.4 %).

Spectra data of complex **TFRS-1**: MS (FAB, ^{102}Ru): m/z 771 ($\text{M}+1$)⁺. ^1H NMR (400 MHz, d-DMSO, 298 K): δ 8.95 (s, 1H), 8.14 (d, $J = 6.0$ Hz, 1H), 7.99 (d, $J = 8.0$ Hz, 1H), 7.83 (t, $J = 8.0$ Hz, 1H), 7.78 (d, $J = 5.2$ Hz, 1H), 7.28 (s, 1H), 7.21 (t, $J = 6.0$ Hz, 1H), 7.64 (d, $J =$

5.2 Hz, 1H).

Synthesis of TFRS-2 and TFRS-3

A similar procedure was conducted as described for **TFRS-1**, starting from 5-hexylthiophene pyridyl pyrazole and 5-hexyl [2,2']bithiophene pyridyl pyrazole. The functionalized sensitizers **TFRS-2** and **TFRS-3** were obtained as the sole product in 27 and 35 % yields, respectively.

Spectra data of complex **TFRS-2**: MS (FAB, ^{102}Ru): m/z 1103 ($\text{M}+1$) $^+$. ^1H NMR (d_6 -DMSO, 400MHz) δ : 8.96 (s, 2H), 8.27 (d, J = 6.4 Hz, 2H), 8.22 (s, 2H), 7.79 (d, J = 6 Hz, 2H), 7.74 (d, J = 3.2 Hz, 2H), 7.45 (s, 2H), 7.42 (d, J = 6 Hz, 2H), 7.05 (d, J = 6 Hz, 2H), 6.96 (d, J = 3.2 Hz, 2H), 2.82 (t, J = 7.2 Hz, 4H), 1.61 ~ 0.83 (m, 22H). Anal. Calcd for $\text{C}_{50}\text{H}_{46}\text{F}_6\text{N}_8\text{O}_4\text{RuS}_2\cdot\text{H}_2\text{O}$: C, 53.61; N, 10.00; H, 4.32. Found: C, 53.93; N, 9.79; H, 4.36.

Spectra data of complex **TFRS-3**: MS (FAB, ^{102}Ru): m/z 1267 ($\text{M}+1$) $^+$. ^1H NMR (d_6 -DMSO, 400MHz) δ : 8.94 (s, 2H), 8.28 ~ 8.26 (m, 4H), 7.86 (d, J = 3.6 Hz, 2H), 7.79 (d, J = 6 Hz, 2H), 7.48 ~ 7.52 (m, 4H), 7.34 (d, J = 3.6 Hz, 2H), 7.20 (d, J = 3.6 Hz, 2H), 7.07 (d, J = 6.4 Hz, 2H), 6.83 (d, J = 3.6 Hz, 2H), 2.76 (t, J = 7.6 Hz, 4H), 1.61~1.24 (m, 16H), 0.83 (t, J = 7.2 Hz, 6H). Anal. Calcd for $\text{C}_{58}\text{H}_{50}\text{F}_6\text{N}_8\text{O}_4\text{RuS}_4\cdot 4\text{H}_2\text{O}$: C, 52.05; N, 8.37; H, 4.37. Found: C, 52.28; N, 8.28; H, 4.28.

Device fabrication

Transparent TiO_2 paste was prepared using published procedures.¹ The transparent TiO_2 thin film with thickness of 12 μm was first deposited on Fluroine-doped tin oxide (FTO). This film was dried at 120 °C for 5 min and then a 5 μm thick layer of 400 nm TiO_2 particles (Solaronix, Ti-Nanoxide 300) was deposited again by screen printing method to form a square with dimension of 0.38 × 0.38 cm². The TiO_2 electrodes were gradually heated under an air flow at 325°C for 5 min, followed by 375°C for 5min, 450°C for 15min, and 500°C for 15 min. The TiO_2

electrodes were treated with TiCl_4 at 70°C for 30 min and sintered at 500°C for another 30 min. After cooling to 80 °C, the TiO_2 electrode was immersed into the dye solution (0.3 mM) containing 10% DMSO in acetonitrile and tert-butyl alcohol (volume ratio: 1:1) for 18 h. The Pt counter electrodes were prepared by spin-coating an H_2PtCl_6 solution (2 mg of Pt in 1 mL isopropyl alcohol) on FTO plates, followed by sintering at 400 °C for 15 min. The dye adsorbed TiO_2 electrodes and the Pt counter were assembled into a sandwich-type cell by heating at 80 °C using a hot-melt ionomer film (Surlyn 1702, 25 μm) as a spacer between the electrodes. The electrolyte solution containing 0.60M butylmethyimidazolium iodide (BMII), 0.03 M I_2 , 0.10 M guanidinium thiocyanate, and 0.50 M *tert*-butylpyridine in the mixed solvent of acetonitrile and valeronitrile with volume ratio of 85:15 (A6141),² was then injected into the cell through a drilled hole in the back of the counter electrode. Finally, the hole was sealed using a hot-melt ionomer film and a cover glass.

Photovoltaic Characterization.

A 150 W xenon light source (Oriel, U.S.A.) was used to give an irradiance of 100 mW cm^{-2} (the equivalent of one sun at air mass (AM 1.5) at the surface of solar cells). Various incident light intensities were regulated with wavelength neutral wire mesh attenuators. The current-voltage characteristics of the cell under these conditions were obtained by applying external potential bias to the cell and measuring the generated photocurrent with a Keithley model 2400 digital source meter (Keithley, U.S.A.). A similar data acquisition system was used to control the incident photon-to-collected electron conversion efficiency measurement. Under full computer control, light from a 150W xenon lamp (Oriel, U.S.A.) was focused through a monochromator onto the photovoltaic cell under test. The monochromator was incremented through the visible spectrum to generate the IPCE (λ) as defined by $\text{IPCE}(\lambda) = 12400(J_{sc}/\lambda\varphi)$, where λ is the wavelength, J_{sc} is short-circuit photocurrent density (mA cm^{-2}), and φ is the incident radiative flux (mW cm^{-2}). Photovoltaic performance was measured by using a black tape as mask with an aperture area of

0.144cm².

Electrical Impedance Measurements.

Electrical impedance experiments were carried out with a PARSTAT 2273 (AMETEK Princeton Applied Research, U.S.A.) electrochemical workstation, with a frequency range of 0.05 – 10⁶ Hz and a potential modulation of 5 mV.

Computational Methodology.

Restricted formalism was adopted in the singlet state geometry optimizations for all studied complexes using the density functional theory (DFT) with B3LYP hybrid functional.³ A "double- ζ " quality basis set consisting of Hay and Wadt's effective core potentials (LANL2DZ)⁴ was employed for Ru atom, and a 6-31G* basis set,⁵ for H, C, O, N, F and S atoms. The relativistic effective core potential (ECP) replaced the inner core electrons of Ru(II) metal atom, leaving the outer core (4s²4p⁶) electrons and the 4d⁶ valence electrons to be concerned. Time-dependent DFT (TDDFT) calculations using the B3LYP functional were then performed based on the optimized structures at ground states.⁶ Oscillator strengths were deduced from the dipole transition matrix elements (for singlet states only). All calculations were carried out using Gaussian 03.⁷

References:

- [1] P. Wang, S. M. Zakeeruddin, P. Comte,; R. Charvet, R. H. Baker and M. Grätzel, *J. Phys. Chem. B*, 2003, **107**, 14336.
- [2] T. Bessho, E. Yoneda, J.-H. Yum, M. Guglielmi, I. Tavernelli, H. Imai, U. Rothlisberger, M. K. Nazeeruddin and M. Grätzel, *J. Am. Chem. Soc.*, 2009, **131**, 5930-5934.
- [3] (a) C. Lee, W. Yang, R. G. Parr, *Phys. Rev. B* **1988**, *37*, 785. (b) A. D. Becke, *J. Chem. Phys.* **1993**, *98*, 5648.
- [4] (a) P. J. Hay, W. R. Wadt, *J. Chem. Phys.* **1985**, *82*, 270. (b) W. R. Wadt, P. J. Hay, *J.*

- Chem. Phys.* **1985**, *82*, 284.; (c) P. J. Hay, W. R. Wadt, *J. Chem. Phys.* **1985**, *82*, 299.
- [5] P. C. Hariharan, J. A. Pople, *Mol. Phys.* **1974**, *27*, 209.
- [6] (a) C. Jamorski, M. E. Casida, D. R. Salahub, *J. Chem. Phys.* **1996**, *104*, 5134. (b) M. Petersilka, U. J. Grossmann, E. K. U. Gross, *Phys. Rev. Lett.* **1996**, *76*, 1212. (c) R. Bauernschmitt, R. Ahlrichs, F. H. Hennrich, M. M. Kappes, *J. Am. Chem. Soc.* **1998**, *120*, 5052. (d) M. E. Casida, *J. Chem. Phys.* **1998**, *108*, 4439. (e) R. E. Stratmann, G. E. Scuseria, M. J. Frisch, *J. Chem. Phys.* **1998**, *109*, 8218.
- [7] Gaussian 03, revision C.02; Gaussian, Inc., Wallingford CT, **2004**.

States	λ_{cal}	f	Assignments
S_{10}	445.9	0.0155	HOMO-4→LUMO (37%) HOMO-1→LUMO+2 (24%) HOMO-3→LUMO (18%) HOMO-1→LUMO+4 (6%)
S_{11}	445	0.0223	HOMO-4→LUMO (56%) HOMO-3→LUMO (16%) HOMO-1→LUMO+2 (7%) HOMO-1→LUMO+4 (5%)
S_{12}	441.1	0.0051	HOMO-1→LUMO+3 (90%)
S_{13}	433.9	0.0271	HOMO→LUMO+4 (90%)
S_{14}	421.5	0.1153	HOMO-1→LUMO+4 (79%) HOMO-2→LUMO+3 (8%)
S_{15}	411.7	0.2729	HOMO-2→LUMO+2 (91%)

Table S1. The Calculated wavelength (λ), oscillator strength (f) and orbital transition analyses of **TFRS-2**.

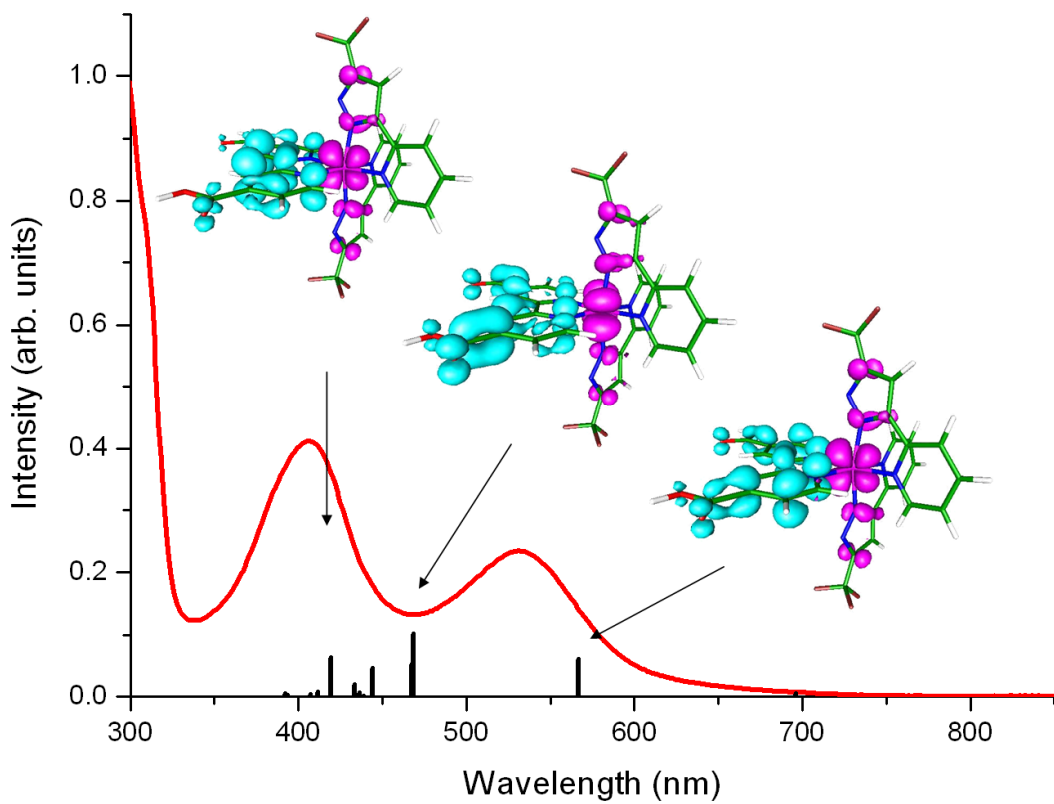


Figure S1. UV-vis experimental absorption spectra of **TFRS-1** measured in DMF solution. Black bars represent the computed vertical electronic excitation intensities (f) by TDDFT method. For three selected optically active electronic transitions (black bars at 567, 468, and 419 nm, respectively) the electron-hole density plots are shown (hole and excited electron densities are represented in pink and cyan, respectively).

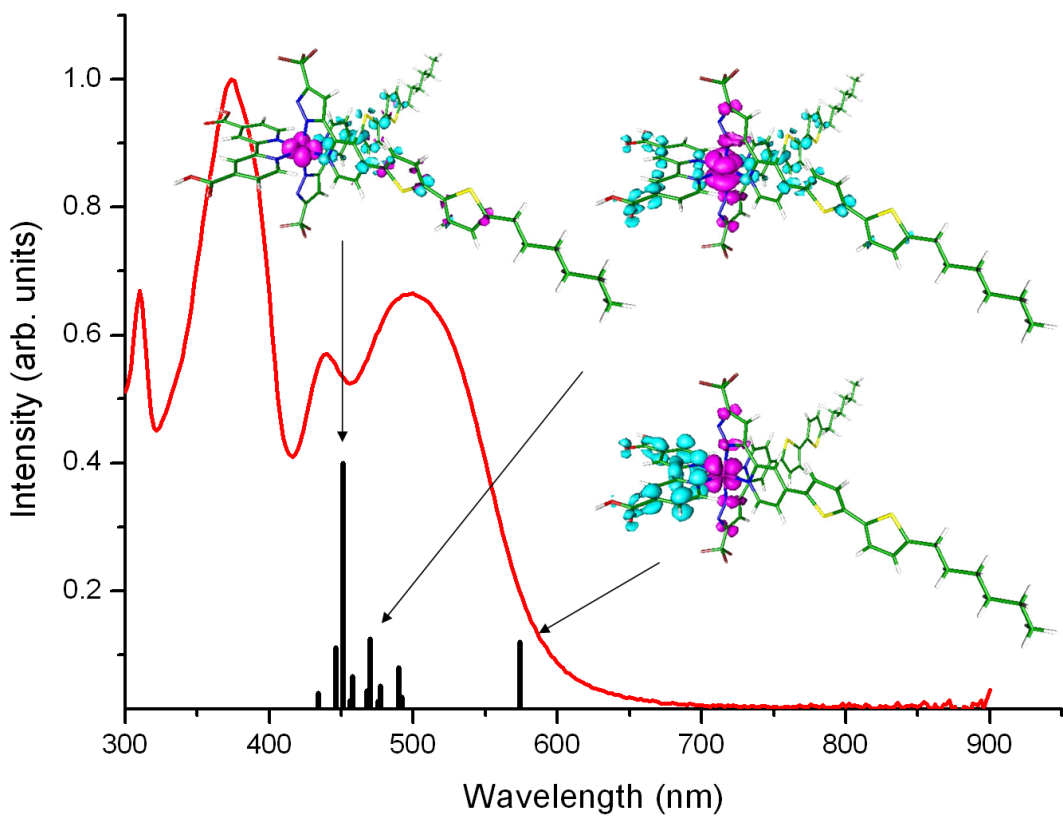


Figure S2. UV-vis experimental absorption spectra of **TFRS-3** measured in DMF solution. Black bars represent the computed vertical electronic excitations intensities (f) by TDDFT method. For three selected optically active electronic transitions (black bars at 574, 470, and 451 nm, respectively) the electron-hole density plots are shown (hole and excited electron densities are represented in pink and cyan, respectively).

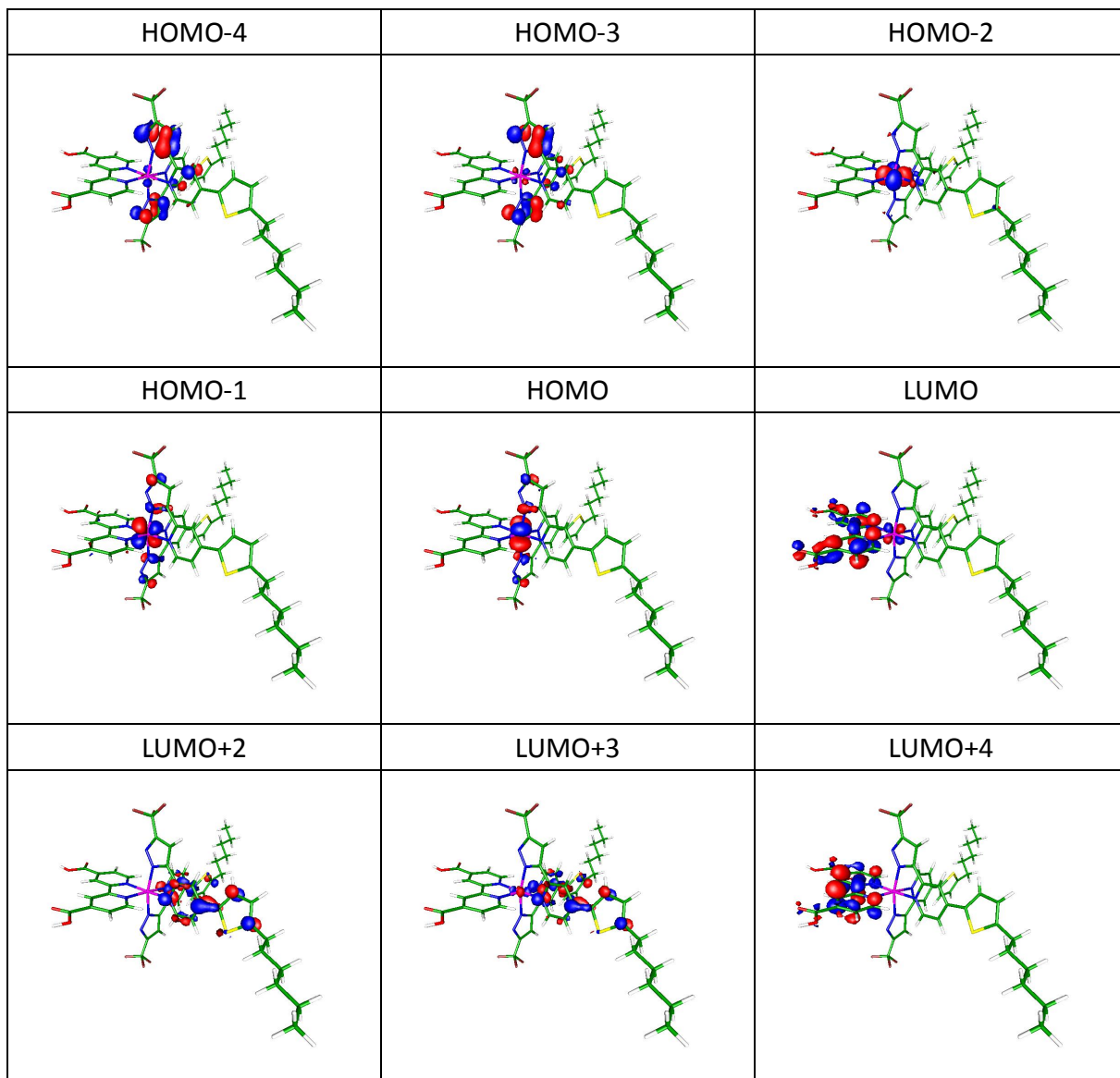


Figure S3. The frontier orbitals involved in the $S_{10} - S_{15}$ electronic transitions of TFRS-2.

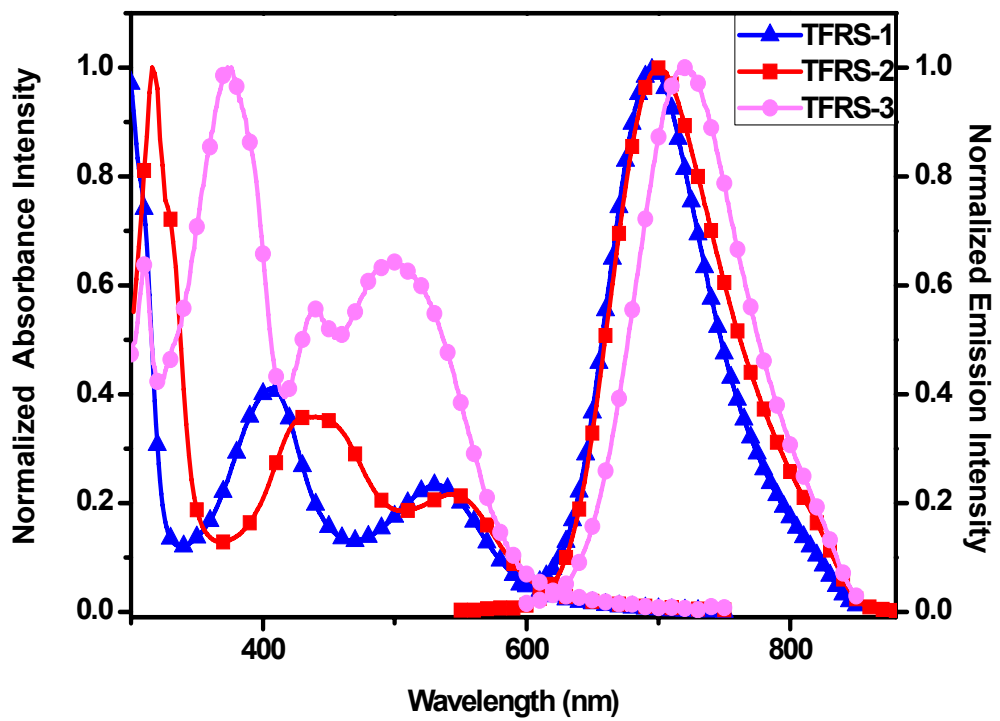


Figure S4. UV-vis absorption and emission spectra of **TFRS-1**, **2** and **3** measured in DMF solution.

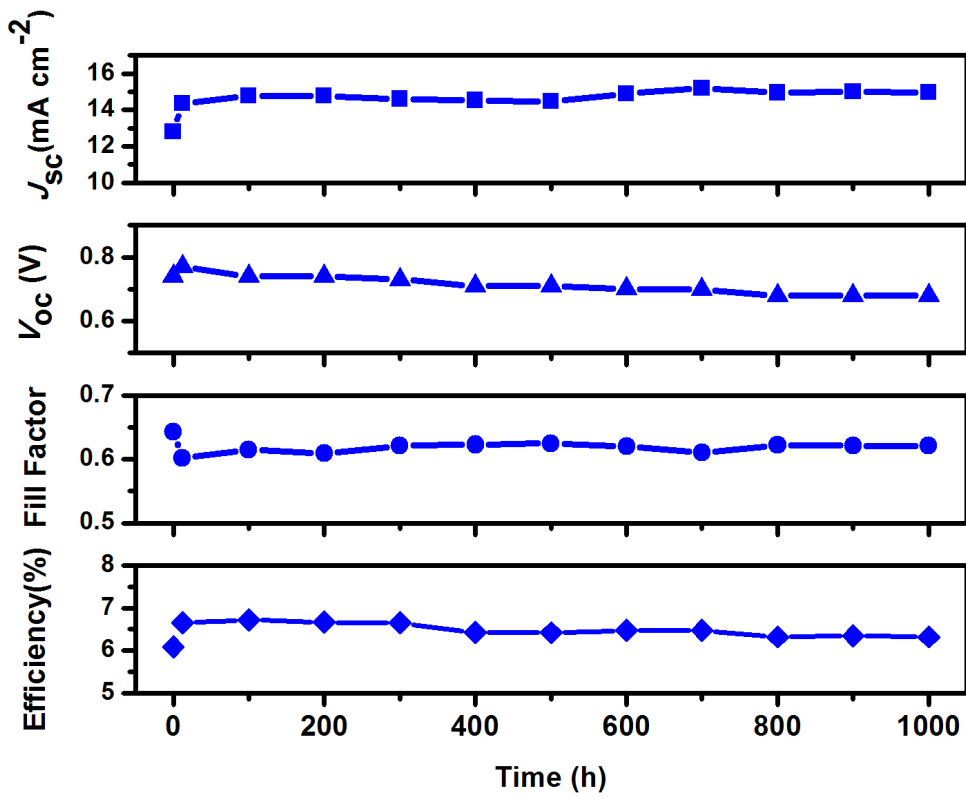


Figure S5. Evolution of solar cell parameters of **TFRS-2** measured under the irradiance of AM 1.5 G sunlight soaking at 60 °C. A 405 nm cut-off long pass filter was put on the cell surface during illumination. Electrolyte: 1.0 M DMPII, 0.5 M iodine, 0.1 M GuNCS, and 0.5 M NMBI (N-methylbenzimidazole) in 3-methoxypropionitrile.